Thin–Walled Structures 115 (2017) 264–276

Contents lists available at ScienceDirect

Thin-Walled Structures

journal homepage: www.elsevier.com/locate/tws

Full length article

Local buckling behaviour of thin-walled members with curved cross-section parts

Dávid Jobbágy, Sándor Ádány*

Budapest University of Technology and Economics, Department of Structural Mechanics, Műegyetem rkp. 3, 1111 Budapest, Hungary

ARTICLE INFO

Keywords:
Curved cross-section
Local buckling
Shell-like behaviour
Capacity prediction

ABSTRACT

In this paper the buckling behaviour of thin-walled members with cross-sections with curved parts is investigated. Due to the curved parts, shell-like buckling is a potential mode of failure. The objective of the research is to understand whether shell-like buckling behaviour might be governing in practical cold-formed steel members. For this aim, numerical studies have been carried out, involving linear buckling analysis as well as nonlinear shell finite element analysis with imperfections, by considering a large number of various cross-sections. Standardized capacity prediction has also been completed, based on elastic critical loads by using the direct strength method, and the results have been compared to that of shell finite element analyses. Based on the results it is concluded that shell-like behaviour might be critical in certain cases, but only in case of unusual cross-section geometries. It was also found that the simple direct strength capacity prediction can reasonably be used in most of the cases.

1. Introduction

As linear cold-formed steel profiles have become everyday solutions in many applications (e.g., purlins, rafters), several research activities started with aiming to develop more efficient cross-sections. These research and/or innovation activities led to more refined cross-section shapes, e.g. with multiple longitudinal stiffeners. Lately, attempts for a more formal mathematical optimization have been reported by various research groups, see e.g. [1–10]. Though these research activities are different in many aspects (e.g., different objective functions are used, different optimization techniques are used, different topologies are considered, etc.), still they share a few important common features. First, practically all of them use the Direct Strength Method (DSM) [11] for capacity prediction, which, at least formally, can be applied to virtually any cross-section geometries, even if its safe applicability has been proved for only certain (so-called pre-qualified) cross-sections. Another common feature is that the found optimal cross-section shapes tend to consist of curved parts rather than flat parts, at least if no special constraints are used to avoid the formation of curved parts. Though from a different root (namely: trying to improve seismic capacity of thin-walled sections for moment resisting frames) and without formal mathematical optimization, researches in [12,13] also concluded that cold-formed lipped channel sections with curved flanges are superior to the classic flat-flange C sections.

Obviously, the highly curved cross-section shapes might be impractical. That is why many of the above-mentioned research groups provided optimal shapes also with considering some production and/or construction constraints, preventing or only partially allowing the formation of curved parts in the optimized cross-section. Based on all these results, it is reasonable to assume that some combination of flat and curved parts might be feasible and advantageous, e.g., by assuming some classical cross-section, but with unusually large corner radii.

The problem is, however, that the behaviour of thin-walled members with curved cross-section parts is not yet investigated in a comprehensive manner, therefore it is questionable whether the reported optimal cross-sections are properly analysed by considering all possible failure modes. Two potential problems might be mentioned. First, it is questionable whether DSM can properly be used to predict the design capacity of cross-sections with curved parts. Second, since curved cross-section parts mean cylindrical surfaces, shell-like behaviour is theoretically possible, but shell-like behaviour is certainly not considered by DSM (and in fact by any current design procedure for cold-formed steel members). This second question might be especially important. Though plate-like and shell-like buckling are geometrically similar, both being associated with small buckling waves, they might have significantly different post-buckling behaviour: plate-like buckling has typically considerable post-buckling reserve (i.e., the load-bearing capacity might be considerably above the critical load), in case of shell-like behaviour, however, the capacity is typically much smaller than the critical load. Therefore, if shell-like behaviour is physically possible but

* Corresponding author.
E-mail address: sadany@epito.bme.hu (S. Ádány).

http://dx.doi.org/10.1016/j.tws.2017.02.026
Received 9 January 2017; Received in revised form 22 February 2017; Accepted 23 February 2017

not considered by the design procedure, the design might be highly unsafe and the so-optimized cross-sections might not be optimal.

Since according to the knowledge of the authors this problem has not yet been addressed, a small research program has been completed to get a basic understanding (i) whether cross-sections with curved parts can be analysed by DSM, and (ii) whether shell-like failure of cold-formed steel members is a failure mode to be considered. Based on the results we might also have basic knowledge whether cold-formed steel members with curved parts can be beneficial to use, compared to typical quasi-sharp cornered cross-sections. Some preliminary results of this research program have been reported in [14,15], while in this paper the whole research program is briefly summarized.

First the numerical studies are presented, completed by shell finite element analysis. Both column and beam members are investigated, considering two cross-section topologies, but a large number of curved and non-curved cross-sections, by systematically changing the corner radii in a wide range. Linear buckling analysis (Section 3), as well as geometrically nonlinear analysis (Section 4) and geometrically and materially nonlinear analysis with imperfections are presented (Section 5). The results are evaluated in the light of some current design procedure, namely Eurocode 3 [16–18] and the direct strength method of the North American Specification (NAS) for cold formed steel structural members [19] (Section 6). Finally, based on the completed calculations and comparisons conclusions are drawn.

2. Overview of the completed research

2.1. Overview

The objective of the research is to check whether shell-like buckling can or cannot be governing in case of thin-walled cold-formed steel column and beam members. In other words, we want to check whether the presence of curved parts in the cross-section geometry deteriorates the post-buckling reserve of the buckling (i.e., buckling characterized by small waves). The aim is not to investigate specific products, but to analyse the phenomena. Therefore, only simple cross-section geometries are selected. One single cross-section topology is chosen for pure compression, and another one for pure bending. The topology for compression is a doubly-symmetrical hollow section shape, (with a maximum dimension of 100 mm,) while the topology for bending is a C-like singly-symmetrical open cross-section shape (with 100 mm width and 130 mm height). It is to note that this slightly unusual lipped-channel geometry is selected in order to eliminate distortional buckling and to be able to investigate cross-sections with very large corner radii. Also, in most of the cases this geometry prevents the plate buckling of the lip, though this phenomenon is not totally excluded. Since the emphasis is on the curved parts, within the given topology, the corners are rounded with variable corner radius, the radius varying in between zero (i.e., sharp corners) and the physically possible maximum (i.e., 50 mm). In case of the hollow section, therefore, the increasing radius transforms the shape from a square hollow section (SHS) to a circular hollow section (CHS), as shown in Fig. 1. The figure shows the considered C-like shapes with the changing corner radius, too.

Since the aim here is to analyse buckling with short buckling waves, only short members are considered, with a length equal to 200 or 300 mm, i.e., the length is roughly twice as much as the maximum cross-section dimension. The selection of short member length automatically eliminates the global buckling phenomena. The distortional buckling is not fully eliminated, still, the short member length and the selected cross-section shapes reduce its significance. In case of hollow sections distortional buckling mode theoretically exists, however, the associated critical load is much larger than those belong to local-plate buckling, hence, it is reasonable to assume that the effect of distortional buckling for the considered column problems is negligible. In case of a C-like cross-section distortional buckling is typically important, however, in our cases the flange lips are relatively large, and if such a cross-section is subject to bending, the lips are lightly compressed, hence it is reasonable to assume that distortional buckling and/or lip buckling has minor role.

The final goal of the numerical studies is to estimate the load-bearing capacity of the members with (and without) significant curved parts and then to make a comparison to existing design procedures. In the lack of real experiments, the load bearing estimation is carried out by finite element analysis, using shell finite elements, considering material and geometric nonlinearity with imperfections (i.e. GMNI analysis). Equivalent geometric imperfections are used, taken as properly scaled buckling shapes.

The major steps of the research work are as follows:

- parametric model definition,
- linear buckling analysis for a large number of cases, by systematically changing the model parameters in wide range of the parameters,
- development of a method to numerically and automatically characterize the buckling modes,
- imperfection sensitivity analyses by using elastic material and geometric nonlinear analysis with geometric imperfections (i.e., GNI analysis),
- load bearing capacity estimation with geometrically and materially nonlinear analysis (i.e., GMNI analysis),
- evaluation of the GMNI capacity prediction in the light of direct strength method (DSM) and the Eurocode 3 design procedure.

Based on the results some qualitative and (approximate) quantitative conclusions can be drawn.

2.2. Parametric FE model

For the parametric studies a parametric finite element model was built in Ansys [20]. The geometry of the analysed cross-section topologies is illustrated in Fig. 1. Eight-node quadratic shell elements have been used, with six degrees of freedom at each node. This element is called SHELL281 in Ansys terminology. A relatively fine mesh is used, the total degrees of freedom being approx. 34,000–47,000 in case of the SHS-like sections and 51,000–98,000 in the C-like sections. The size of the equation system was a key factor since thousands of cases have been investigated, therefore, a balance had to be kept in between accuracy and running time. It is to mention that some other finite element types have been tested, too, but it was concluded that there is no significant difference in the results if appropriate mesh density is chosen.

A globally and locally hinged support was defined for both end sections. Warping is practically restrained. One may think of this support arrangement as if thick plates were welded to the end cross-sections, and the plate is supported in one point by a hinge (i.e. by restraining translations and twisting rotation around the longitudinal axis of the member, while allowing the rotations around the other axes). Practically, a master node is defined at each end to which each end cross-section node is linked by rigid constraint equations. It is to note that some slightly different support arrangements were also considered, but it was concluded that it had no any significant influence on the local behaviour.

3. Linear buckling analysis

3.1. Results

Linear buckling analyses are performed for both cross-section topologies, with varying corner radius and thickness. More specifically, the thickness varied from 0.4 mm to 1.0 mm by 0.1 mm steps and from 1.0 mm to 3.0 mm by 0.2 mm steps, while the corner radius varied from zero to the physically possible maximum 50 mm by 5 mm steps. Altogether 685 cases are analysed, and in each case the first 200–300

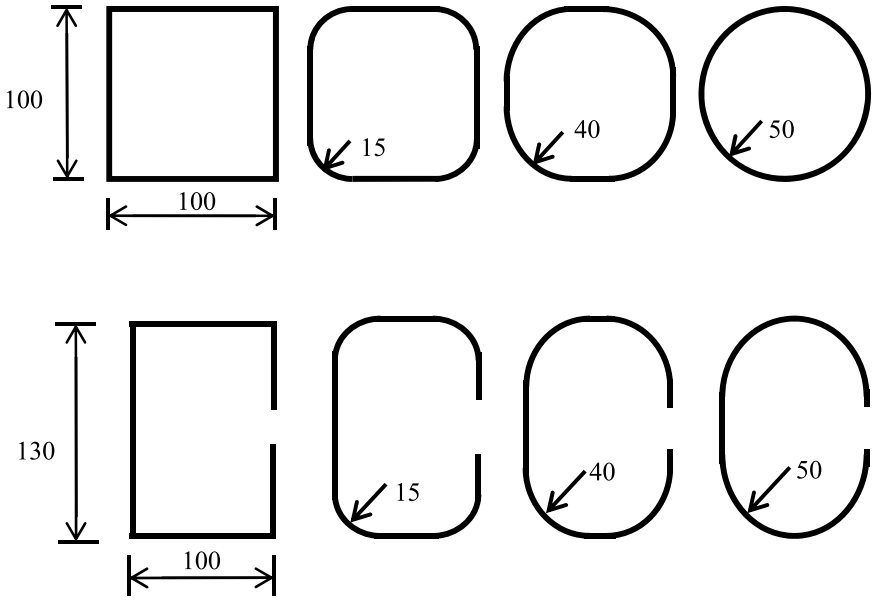

Fig. 1. Cross-sections.

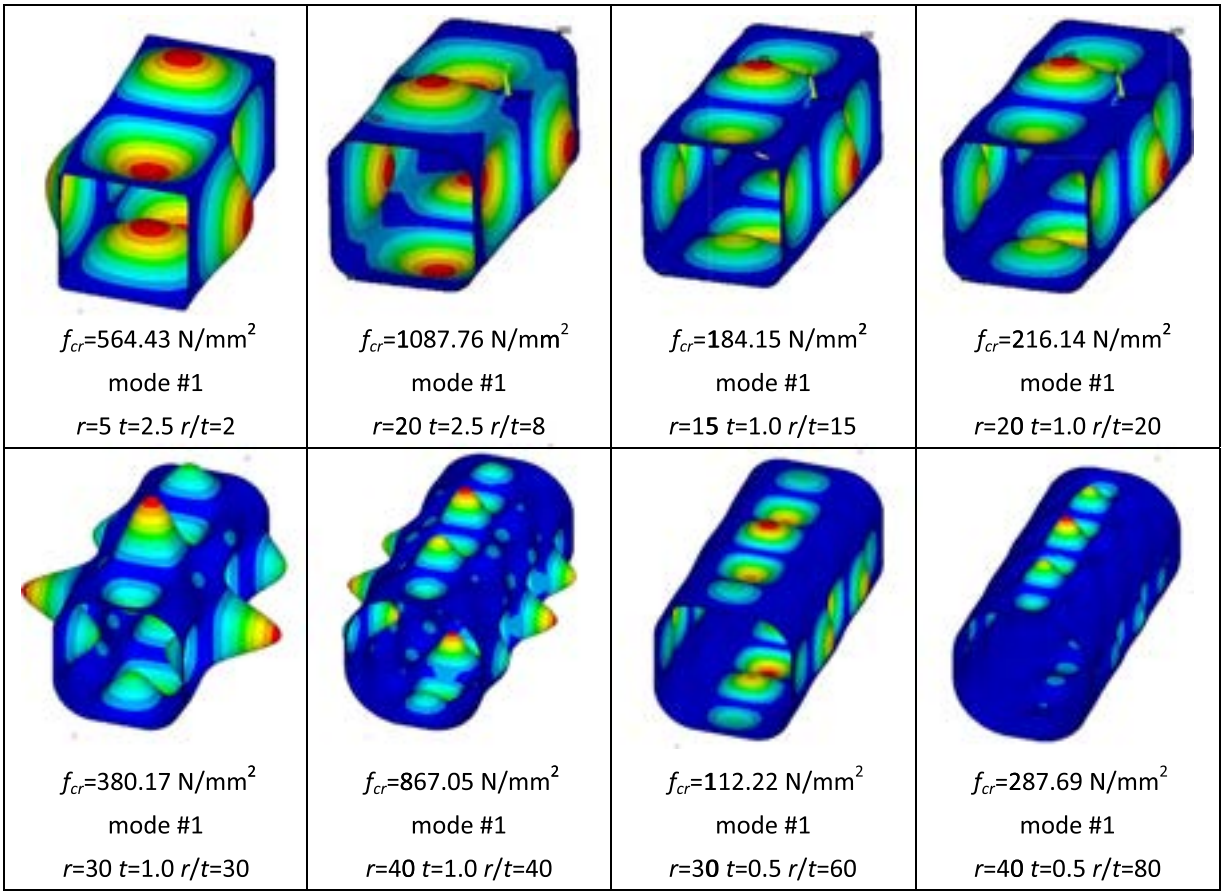

Fig. 2. First buckling modes of SHS sections with various r/t ratios.

critical loads and corresponding buckled shapes are calculated. (Note, in certain cases much more modes are calculated, up to 2–3000 modes.) Since the results are strongly dependent on the r/t ratio of the cross-section, various r/t ratios are considered for illustration, from $r/t=2$ ($r=5$ mm, $t=2.5$ mm) up to $r/t=80$ ($r=40$ mm, $t=0.5$ mm). Some of the buckling modes are shown in Figs. 2–5.

In general, if the deformations are concentrated to the flat parts of the member (while the curved parts are subject to much smaller deformations), the buckled shape is most likely “plate-like” buckling. On the other hand, if significant deformations appear at the curved parts, the buckled shape is most likely “shell-like” buckling. If deformations are important in both the flat and curved parts, the mode is considered as “mixed”.

By the visual inspection of the buckling modes it can be concluded that:

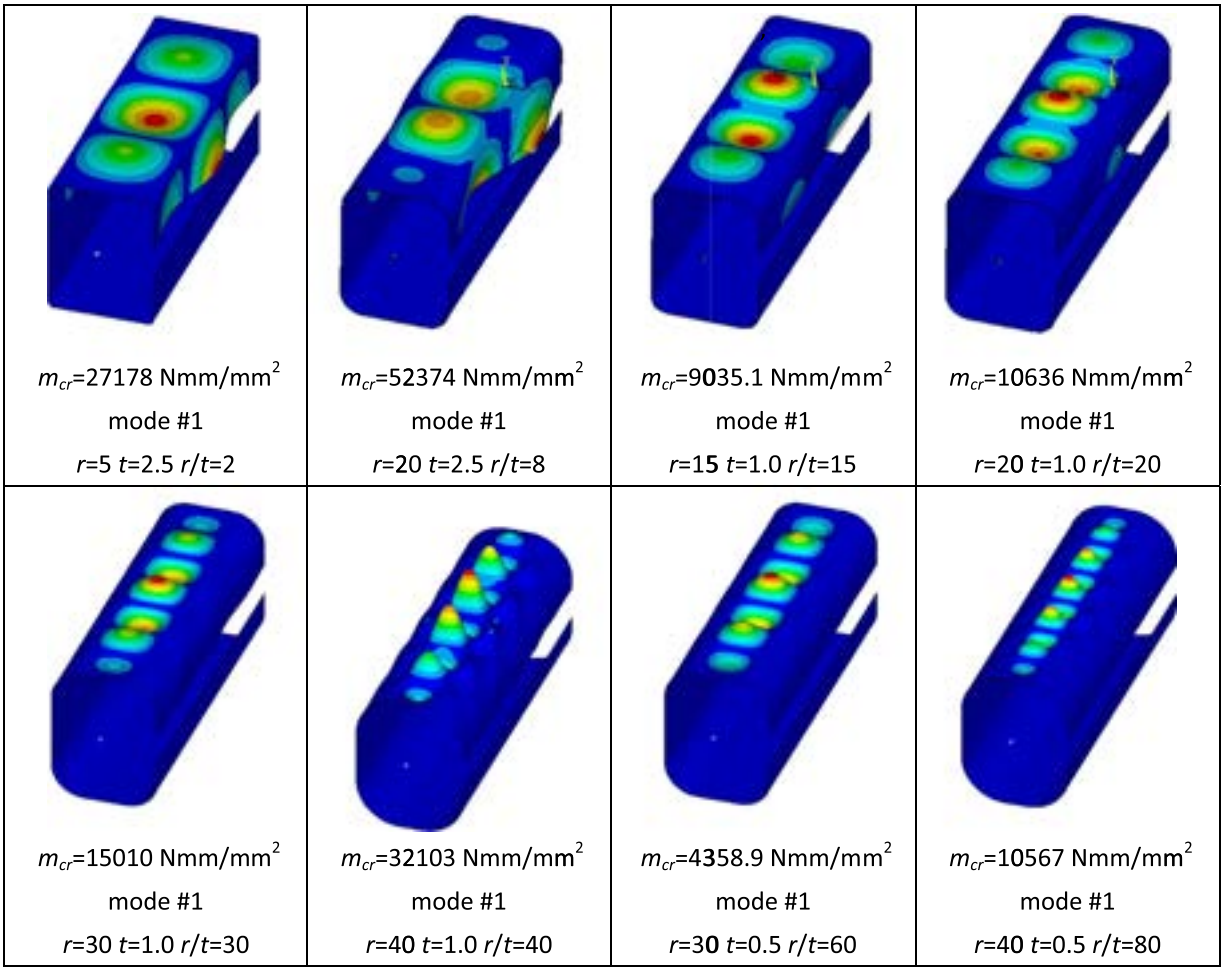

Fig. 3. First buckling modes of C sections with various r/t ratios.

- in case of smaller corner radius the first few hundred buckling modes can be classified as (classic) plate-like modes,
- in case of larger corner radius the first buckling modes are plate-like, but shell-like modes appear among the higher modes,
- the larger the corner radius, the sooner the shell-like buckling appears,
- axisymmetric shell-type (see Fig. 4, #158) modes appear, too, however, axisymmetric modes are found only as very high modes and/or in case of very large corner radius,
- the increasing tendency of the critical loads are dependent on the cross-section shape: the larger the corner radius, the slower the increasing of the critical loads (e.g., in case of a hollow section with $t=1.0$ mm, the ratio of the 200th to the 1st critical load is 16.8 if $r=5$ mm, while the same ratio is 4.3 if the radius is 40 mm),
- distortional buckling of the beam sections (i.e., buckling with opening-closing of the C-section) is efficiently excluded,
- plate buckling of the lip of the lipped channel sections show up; mostly it is associated with the simultaneous buckling of the flange (see e.g., the first two cases of Fig. 3), but in some cases the buckling waves in the lip are the dominant ones (see e.g. mode #159 in Fig. 5).

3.2. Spectral analysis of buckling shapes

Buckled shapes are intended to be used as geometric imperfections in nonlinear analyses for a large number of cases. It is known that the various buckling modes have very different post-critical behaviour. It is expected, therefore, that the member will show significantly different imperfection sensitivity depending on the nature of the imperfection, i.e., depending on the nature of the buckling mode which is used as geometric imperfection. Since we have many different cross-section shapes, and hundreds of buckling modes for each case, it is highly beneficial to be able to numerically characterize the buckled shapes, which numerical characterization might later be connected to the imperfection sensitivity (or: post-critical behaviour).

Here a simple and automatic characterization is proposed and used, which can be summarized as follows:

- longitudinal straight lines are defined at some characteristic points of the member,
- the displacements along the lines are collected,
- the displacement function along each line is approximated by trigonometric series,
- the coefficients of interpolation functions are normalized.

Since in most of the cases only a few coefficients have non-zero values, the few non-zero coefficients show the characteristic buckling lengths, as well as highlight those parts of the member where the deformations are dominant.

To illustrate the spectral analysis of the buckling shapes, a hollow section with $r=40$ mm and $t=1$ mm is considered here, with the 3 buckling modes shown in Fig. 2 and Fig. 4. The straight lines are defined as shown in Fig. 6, namely: two in the flat part of the cross-section (f1,f2), and two in the curved part (c1,c2). Fig. 7 shows the normalized coefficients (i.e., the participation of the given wave-length) for the 4 lines.

It can be observed that

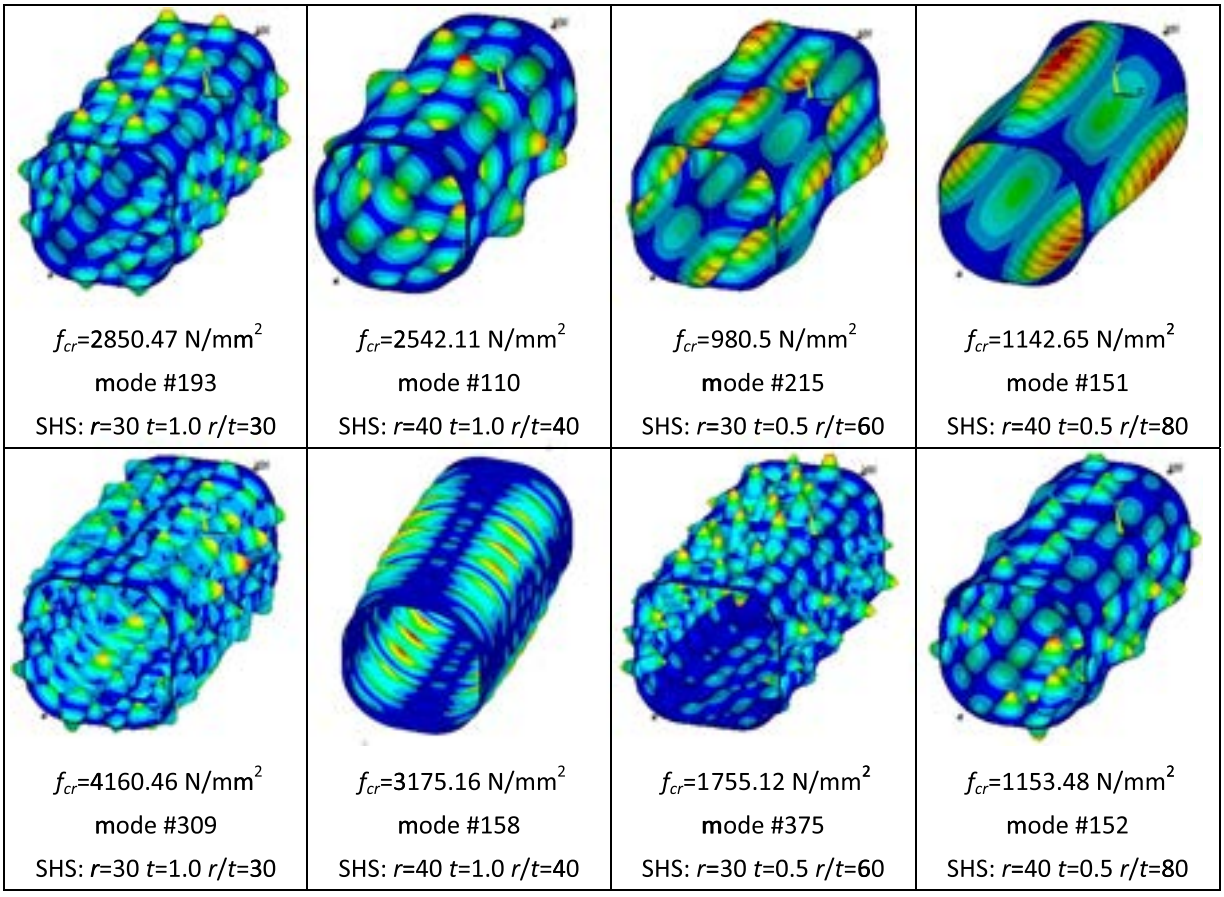

Fig. 4. Sample buckling modes of SHS sections with significant waves in the curved parts.

- mode #1 is clearly plate-like buckling, since waves of significant amplitude occur in the flat parts (f1,f2), with characteristic wave-lengths of 33 mm and 25 mm, while the curved parts practically remain undeformed,
- mode #158 is clearly shell-like buckling, since waves of significant amplitude occur in the curved parts (c1,c2), with characteristic wave-lengths of 12.5 mm and 11 mm, while the flat parts practically remain flat,
- mode #110 shows both plate-like and shell-like characteristics, since there are waves of significant amplitude in both the flat (f1,f2) curved (c1,c2) parts, the characteristic wavelengths being 67 mm and 40 mm (though with some contribution from shorther wave-lengths, too).

It can be concluded, therefore, that the here-introduced spectral analysis of the buckled shapes makes it possible to formally categorize the buckling modes, i.e., to define whether the given buckling mode is plate-like, shell-like or mixed. This categorization does not require visual inspection, hence, it is automatic (for the given cross-section topologies). By the application of this spectral analysis it is straightforward to select a buckling mode of the desired type as geometric imperfection in nonlinear analyses.

4. Elastic analyses of imperfection sensitivity

In order to learn the sensitivity of the members to various geometric imperfections, through which the post-critical behaviour can also be explored, various buckling modes are used as geometric imperfections in nonlinear analyses. Both elastic and materially nonlinear analyses have been performed. First the elastic analyses are discussed.

In the frame of the elastic nonlinear analyses the imperfection sensitivity of both hollow and C sections are studied. Various corner radii have been considered. In order to reduce the number of cases, one single thickness is assumed (t = 1.0 mm), and for each radius only three imperfection shapes are applied, namely a plate-like, a mixed, and a shell-like. These imperfect shapes are selected from the linear buckling shapes, by using the spectral analysis as discussed above. The buckled shapes are scaled so that the maximum out-of-plate displacement would be equal to 0.05, 0.1, 0.15, 0.2, 0.4, 0.5, 0.75, 1.0, 1.5, 2.0, 3.0, and 4.0 mm, respectively. This means that a very wide range of imperfection amplitudes has been considered.

The geometric non-linear elastic analyses (i.e., GNI) load-displacement curves are established. The analyses have been controlled by the prescribed axial displacements, while the load has been calculated as reaction force at the supports. The maximum point of the load-displacement curve (if exists and found during the analysis) can be considered as the elastic load-bearing capacity of the member. As known, the elastic capacity can be quite different from the elastic critical load, the difference being dependent on the nature of buckling: in case of plate-like buckling significant post-buckling reserve might exist, (i.e. the capacity can be larger than the critical load), while in case of shell buckling the capacity is typically much smaller than the critical load. However, the actual capacity is also dependent on the initial magnitude of the imperfection. Some samples of load-displacement curves are presented in Fig. 8.

By having the load-displacement curves for the various cases, the relationship in between the imperfection shape (i.e. buckling mode), imperfection magnitude and elastic capacity can (theoretically) be established. Though the analyses can technically be fully automated, the detailed evaluation of the results highlights the difficulties and limits of this type of finite element calculation. In many cases a sudden change of the deformed configuration occurs as the load is increasing. If

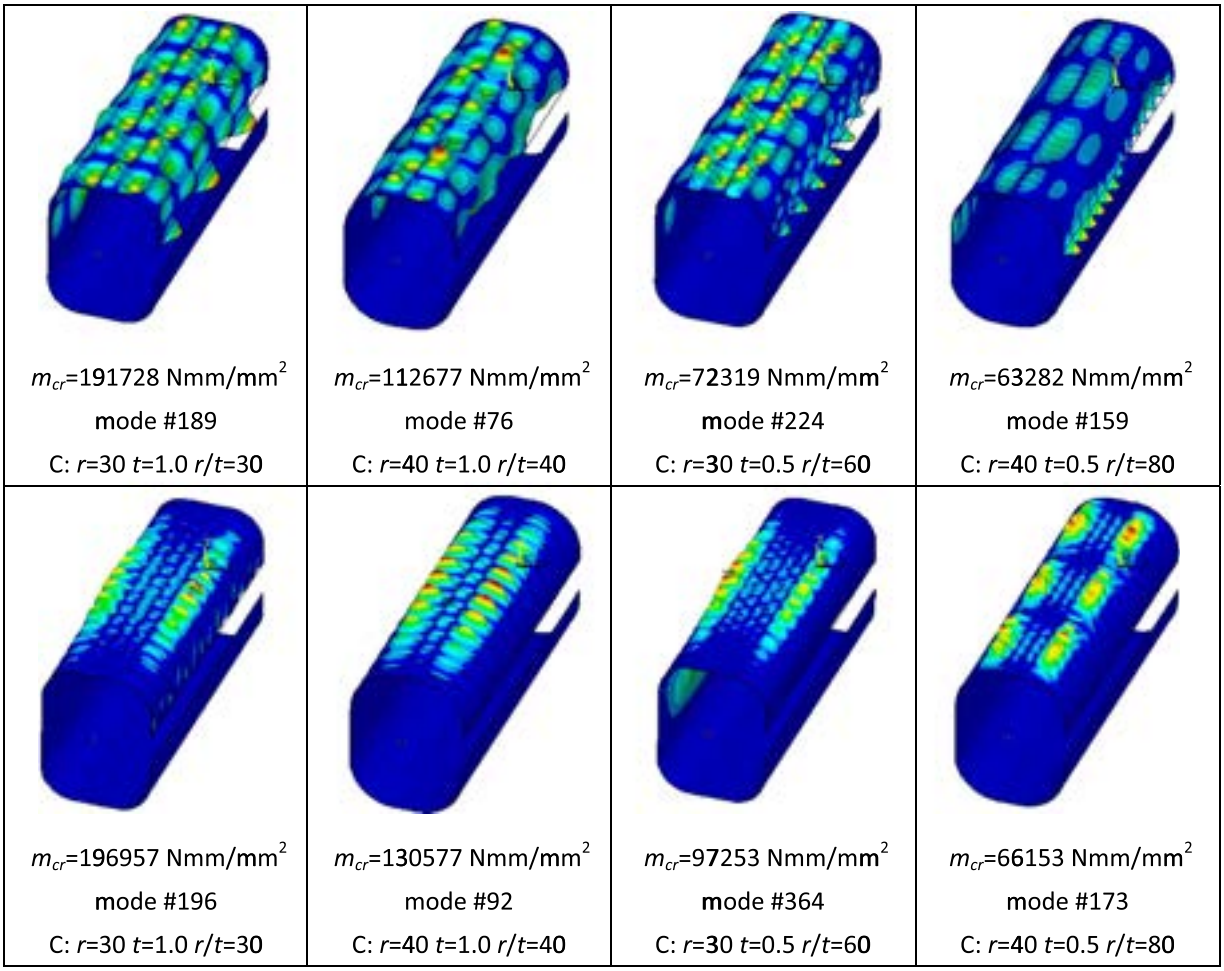

Fig. 5. Sample buckling modes of C sections with significant waves in the curved parts.

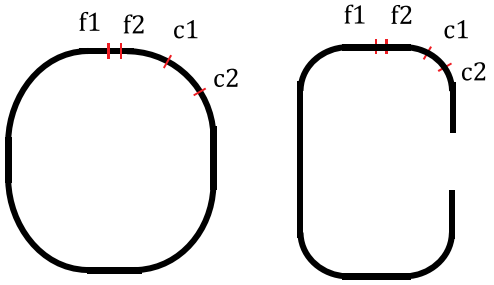

Fig. 6. Positions of longitudinal lines for spectral analysis of buckling shapes.

this snap occurs, the calculated capacity (though technically correct) does not belong to the original imperfection, therefore, the calculated capacity cannot be used to characterize the member sensitivity to the initially considered imperfection shape. It is also observed that this snap phenomenon is typical if the initial imperfection magnitude is small, and becomes rarer as the imperfection magnitude increases. In Fig. 9 this phenomenon is illustrated, where load-displacement curve is plotted for a hollow section with $r=0$ mm and $t=1$ mm, by using buckling mode #10 as imperfection but with a very small initial magnitude (0.005 mm). Some typical deformed shapes are also presented, belonging to various points of the curve, as marked.

As a consequence of this snapping phenomenon, automatic evaluation of the results is questionable, since it is practically impossible to properly assign the elastic capacities and initial imperfections. In the lack of a reliable automatic evaluation process the imperfection sensitivity is established only for a few characteristic cases, by manually checking the non-linear behaviour during the whole load incremental process. In Fig. 10 the imperfection sensitivity is illustrated for a hollow section with $r=40$ mm and $t=1$ mm. It can be observed that (i) plate-like imperfection (e.g., mode #1) leads to elastic capacities larger than the critical load, (ii) if considerable shell-like deformation exists in the imperfection (e.g., mode #110 and #158), the elastic capacity is much smaller than the critical load, (iii) the larger the amplitude of the initial imperfection is, the smaller the elastic capacity is, and (iv) the elastic capacity is not too sensitive to the magnitude of the geometric imperfection.

5. Capacity prediction by GMNI analyses

5.1. Results

To estimate the load-bearing capacity of the members, geometrically and materially nonlinear analyses are carried out. (Note, since the members are short, and global and distortional behaviour are practically excluded, the calculated load-bearing capacity characterizes the local behaviour only.) Since it is known that different imperfection patterns lead to different nominal capacities, parametric study is performed here by considering a large number of possible imperfection patterns. In all the cases, the imperfection pattern is assumed to be in the shape of a linear buckling mode.

The parametric study has been intended to be comprehensive, at least for the selected two cross-section topologies. The varying parameters are the following: the thickness, the corner radius, the imperfection pattern, the imperfection amplitude, and the yield strength of the material. It is realized, however, that a comprehensive parametric study

Hollow section r=40mm, t=1mm												
Buckling shape #1				Buckling. shape #110				Buckling. shape #158				Half-wave length [mm]
Node sets				Node sets				Node sets				
f1	f2	c1	c2	f1	f2	c1	c2	f1	f2	c1	c2	
0	0	0	0	0	4	1	1	0	0	0	0	200
1	1	0	0	0	0	0	0	1	1	0	1	100
0	0	0	0	0	**42**	**18**	**19**	0	0	0	0	67
3	3	0	0	0	0	0	0	1	0	3	0	50
0	0	0	0	0	**100**	**32**	**38**	0	0	0	0	40
100	**85**	2	2	0	0	0	0	0	0	1	0	33
0	0	0	0	0	**16**	1	6	0	0	0	0	29
71	**61**	1	1	0	0	0	0	0	0	1	0	25
0	0	0	0	0	9	1	2	0	0	0	0	22
0	0	0	0	0	0	0	0	0	0	1	1	20
0	0	0	0	0	7	1	1	0	0	0	0	18
0	0	0	0	0	0	0	0	0	0	1	3	17
0	0	0	0	0	7	0	0	0	0	0	0	15
0	0	0	0	0	0	0	0	0	0	4	7	14
0	0	0	0	0	**20**	1	1	0	0	0	0	13
0	0	0	0	0	0	0	0	2	1	**17**	**61**	12.5
0	0	0	0	0	6	0	0	0	0	0	0	12
0	0	0	0	0	0	0	0	4	2	**37**	**100**	11
0	0	0	0	0	1	0	0	0	0	0	0	10.5
0	0	0	0	0	0	0	0	1	0	2	**14**	10

Fig. 7. Wave-length content (%) of buckling shapes of SHS with r=40 mm, t=1.0 mm.

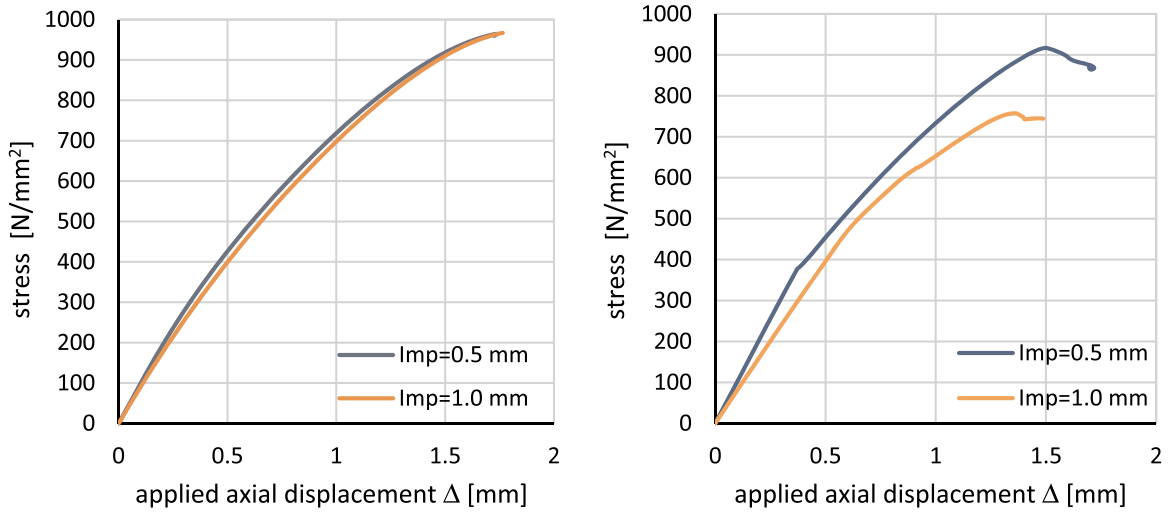

Fig. 8. Load-displacement curves from GNI analyses for SHS section, r=30 mm, t=1.0 mm, with plate-like imperfection shape (left) and shell-like imperfection shape (right).

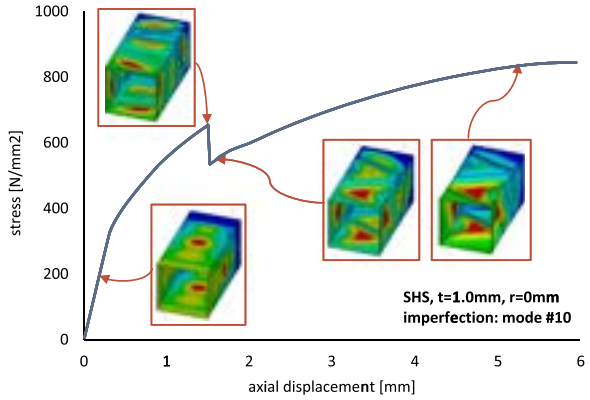

Fig. 9. Load-displacement curves from GNI analyses with snapping phenomenon.

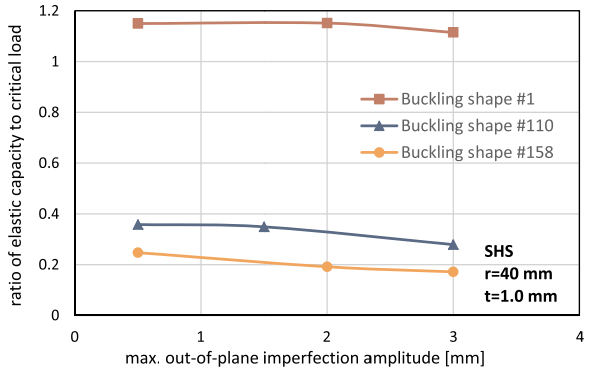

Fig. 10. Calculated imperfection sensitivity of SHS ($r=40$ mm, $t=1.0$ mm).

would require unrealistic computation time, therefore, the parameters are carefully selected, as follows.

Based on some preliminary calculations it was concluded that the yield strength does not affect the tendencies (though the numerical values are obviously affected), thus, it was decided to use one single yield strength value, namely 350 MPa, which is a frequently used basic yield strength for cold-formed steel members.

For the other parameters: we have considered both cross-section topologies, three thickness values: 0.5, 1.0, and 2.5 mm, and (in most of the cases) five corner radius values: 5, 15, 25, 30, and 40 mm.

The number of imperfection patterns may almost be infinite. To have a realistic amount of imperfection patterns, we have selected the first 50–200 linear buckling modes for all the considered cases, plus we have selected the shell-like and mixed modes (by applying the above-described spectral analysis procedure) from the first (maximum) few thousand buckling modes. This selection of imperfection patterns is based on the observation that the first buckling modes are mostly (or exclusively) plate-like modes and the first dozens of plate-like modes will most probably contain the most unfavourable plate-like imperfection pattern, therefore, it is enough to select only the shell-like patterns from the higher modes. Thus, this selection of imperfection patterns ensures that all the potentially most unfavourable patterns will be considered, while the number of considered imperfection patterns remains practically manageable.

As far as imperfection magnitude is concerned, it is known that the general tendency is: the larger the imperfection magnitude is, the smaller the calculated capacity is. However, in many cases the influence of the imperfection magnitude on the calculated capacity is not too significant, at least in the practically important range of possible imperfections. Therefore, our aim was to select a limited number of imperfection magnitudes. In case of plate-like buckling behaviour (of sharp-cornered members), the Eurocode for steel plated elements [16] gives guidance for the determination of the magnitude of the initial equivalent imperfections. In case of shell-like buckling behaviour, at least in case of compressed cylindrical shells, guidance is given in the Eurocode for steel shells [21]. In this latter design standard the value of the imperfection magnitude is greatly dependent on the wall thickness. Finally we have selected one single imperfection magnitude for each considered thickness, as follows: 0.5, 0.7, and 1.5 mm for the thickness of 0.5, 1.0, and 2.5 mm respectively. These values can be regarded as upper limits that are proposed or allowed by the referenced design codes. It is to note, although these values are technically correct, sometimes they seem to be slightly unrealistic, since the half-wave-length of higher buckling modes is normally between 5 and 20 mm (for the considered cases). Still, it is believed that the performed analyses and the results correctly show the behaviour and the tendencies. As far as the actual load-bearing capacities are concerned, the here-presented values can be regarded as realistic estimations (most probably: slightly conservative estimations).

In the GMNI analysis load-displacement curves are established. The analyses have been controlled by the prescribed axial displacements, while the load has been calculated as reaction force at the supports. The nominal capacity is the maximum point of the load-displacement curve. In order to be able to compare the various cross-sections, we have used a normalized version of the capacity, i.e., the maximum normal force or maximum bending moment divided by the cross-sectional area. Samples are shown in Fig. 11.

Calculated normalized capacities are given in Tables 1, 2. Four capacity values are given for all the considered cases, as follows. The value earmarked as “first mode” means the calculated capacity if the first linear buckling mode is used as geometric imperfection. The value of “min of first 10” and “min of first 50” means the minimal capacity of the capacities calculated with the first 10 or 50 buckling modes, respectively. Finally, “min of all” is the minimal capacity value among all the considered geometric imperfections (including very high

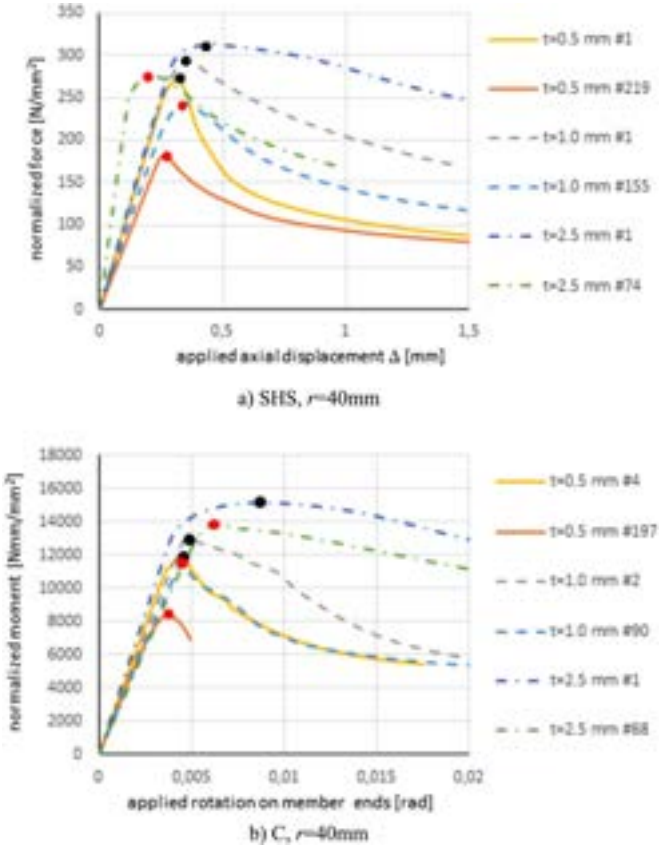

Fig. 11. Sample load-displacement curves from GMNI analyses a) SHS, $r=40$ mm, b) C, $r=40$ mm.

Table 1
GMNI-estimated capacities for SHS-like sections.

t mm	r mm	r/t	Capacity first mode N/mm^2	Capacity min of first 10 N/mm^2	Capacity min of first 50 N/mm^2	Capacity min of all N/mm^2
0.5	5	10	88	83 (10)	83 (10)	79 (1998)
0.5	15	30	151	139 (7)	139 (7)	122 (1106)
0.5	30	60	212	204 (2)	195 (20)	142 (272)
0.5	40	80	273	257 (7)	254 (13)	182 (218)
1.0	5	5	147	147 (1)	142 (19)	142 (19)
1.0	15	15	212	190 (8)	190 (8)	190 (8)
1.0	30	30	253	253 (1)	253 (1)	247 (352)
1.0	40	40	294	292 (8)	292 (8)	243 (155)
2.5	5	2	242	242 (1)	242 (1)	242 (1)
2.5	15	6	257	257 (1)	257 (1)	257 (1)
2.5	30	12	298	297 (7)	294 (46)	254 (139)
2.5	40	16	313	308 (9)	304 (48)	276 (74)

Table 2
GMNI-estimated capacities for C-like sections.

t mm	r mm	r/t	Capacity first mode Nmm/mm^2	Capacity min of first 10 Nmm/mm^2	Capacity min of first 50 Nmm/mm^2	Capacity min of all Nmm/mm^2
0.5	5	10	5093	4511 (8)	4511 (8)	4511 (8)
0.5	15	30	7165	6815 (2)	6535 (22)	6309 (904)
0.5	30	60	9824	8946 (5)	8795 (38)	6779 (325)
0.5	40	80	11,354	10,156 (6)	9361 (29)	8121 (196)
1.0	5	5	8154	8154 (1)	8092 (27)	8092 (27)
1.0	15	15	9032	9032 (1)	8815 (31)	8365 (585)
1.0	30	30	12,005	11,972 (9)	11,972 (9)	10,971 (186)
1.0	40	40	12,950	12,950 (1)	12,838 (42)	11,640 (90)
2.5	5	2	13,420	13,417 (2)	13,417 (2)	13,417 (2)
2.5	15	6	13,210	13,210 (1)	13,210 (1)	13,210 (1)
2.5	30	12	14,419	14,370 (5)	14,370 (5)	14,170 (102)
2.5	40	16	15,147	13,894 (9)	13,644 (31)	13,526 (52)

modes). The number in the bracket indicates the mode number to which the actual (minimal) capacity is associated. Since the first 50 linear buckling modes are always plate-like modes, the value of "min of first 50" can be regarded as an estimation of the capacity that belongs to plate-like behaviour. On the other hand, the value "min of all" can be regarded as an estimation of the capacity (considering any mode as imperfection).

Based on the results of Tables 1, 2, the following observations may be mentioned.

- Taking the first linear buckling mode as geometric imperfection does not always lead to minimal capacity, even if only plate-like behaviour is considered, and even if small corner radii are considered.
- The difference between the values "min of first 10" and "min of first 50" is always small. It means that the capacity prediction based on the first few (say, first 10) buckling modes gives a realistic estimation for the plat-like behaviour of the member. This is especially true for smaller r/t ratios, but approximately true for any of the analysed cases.
- The capacity degrading effect of shell-like buckling exists, but only for small thickness and/or large corner radius. It seems that if the r/t ratio is smaller than 20, shell-like behaviour is never governing, but if the r/t ratio is larger than approx. 20–30, shell-like behaviour could become critical. Obviously, this threshold value of r/t ratio is much larger than the ones of current practical cold-formed profiles, but the optimized cross-sections might have such curved parts.
- The calculated capacity increases with the corner radius even in the case of most unfavourable imperfection patterns and even if shell-like behaviour is considered. Hence, our results, in general, justify the findings of previous researches which suggested that curved cross-sections could be beneficial. Note, however, that in this study only plate-like and shell-like buckling behaviour are considered, while global and distortional buckling are excluded, therefore the observed beneficial effect of the larger corner radii is validated only for the local buckling behaviour.

6. Evaluation of the results in the light of design codes

6.1. Sections with small corner radius

Sections with the smallest analysed corner radius, i.e., $r=5$ mm, are discussed first. These sections are not principally different from practical sections, therefore current design codes can be applied for capacity prediction, at least approximately. Two methods are applied here: effective width method as included in Eurocode 3 [16–18], and direct strength method as included in [19].

It is to note that square hollow sections are covered by Part 1-1 of Eurocode 3 [18], while the lipped channel sections by Part 1–3 of Eurocode 3 [17]. However, in both cases the effective widths due to local-plate buckling are determined by Part 1–5 of Eurocode 3 [16]. It is also to note that in [17] there are two kinds of geometrical limits for the applicability of the rules: one is width-to-thickness ratio values as summarized in Table 5.1, the other is the limit of corner radius as defined in Clause 5.1(6). The width-to-thickness ratios are fully satisfied in case of $t=1.0$ and $t=2.5$ mm thickness, but not fully satisfied in case of $t=0.5$ mm thickness. The maximum radii according to Clause 5.1(6) are 12 mm, 24 mm and 60 mm, for $t=0.5$ mm, 1.0 mm and 2.5 mm, respectively. Since we have applied Eurocode calculations only for $r=5$ mm radius, the criterion for the maximum corner radius is satisfied (but it would be violated by many other considered sections with large corner radius). Since most of the applicability criteria are satisfied for most of the analysed cross-sections, the here presented Eurocode capacity values can be considered as realistic design capacity values.

In the Eurocode calculation the partial factors are assumed to be equal to 1.0, and the nominal thickness is assumed to be equal to the design thickness. In case if bending iteration is performed to find a consistent effective cross-section and stress distribution. The rounded corners are considered by using notional plate widths. The resistance for compressed members (i.e. SHS section) is calculated as the product of effective area and the basic yield strength. The resistance for the members in bending (i.e. C sections) is calculated as the product of effective section modulus and the yield strength. In case of SHS only local buckling is considered, while in case of C sections two capacity values are calculated, one without considering distortional buckling, and one with considering distortional buckling.

In case of DSM the local buckling capacity is predicted (without considering safety factors). The critical stress to local plate buckling is determined by finite strip calculation, using CUFSM [22].

The GMNI calculations are based on initial geometric imperfections. The imperfection amplitude is defined in a simplified and conservative way. It can be suspected that GMNI somewhat underestimates the real capacity, this underestimation is probably larger for the thicker thicknesses. Moreover, the effect of conservative selection of imperfection amplitude is certainly smaller for the bending capacity (i.e., C sections), since in case of bending the half of the section is in tension which is hardly affected by the imperfections. So, it is reasonable to assume that the axial capacity of the 2.5-mm-thick SHS is underestimated by the GMNI analysis, while the other GMNI capacities can be considered as good estimations of the real capacities.

The results are summarized in Fig. 12, where the calculated capacities are plotted as a function of the buckling mode number (used as initial equivalent geometric imperfection).

In case of thin sections in compression a considerable difference is found in between EC3 and DSM. Compared to GMNI, DSM seems to overestimate the capacity, while EC3 seems to slightly underestimate

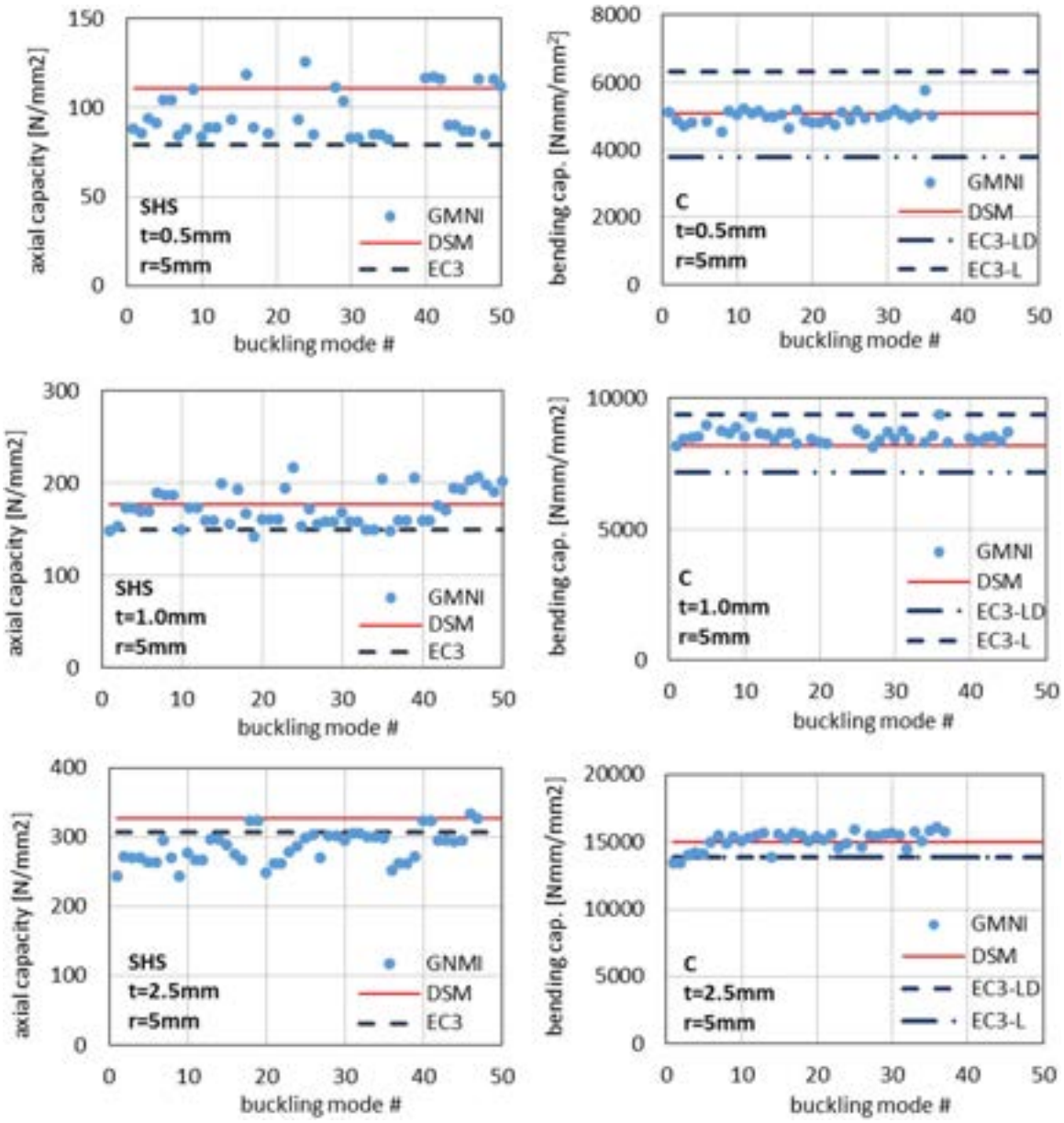

Fig. 12. Comparison of capacities for sections with small radius.

the capacity. In case of thicker sections, or in case of bending, the difference between EC3 and DSM capacity prediction is much smaller.

In case of members in bending, the section geometry has been selected so that distortional buckling would have no significant effect. Still, the EC3 design procedure finds important effect of distortional buckling in case of $t=0.5$ mm and $t=1.0$ mm. Compared to the results of DSM and GMNI, it can be assumed that for the actual (unusual) cross-section geometries the applied EC3 procedure overestimates the importance of distortional buckling. It is to observe, that in case of members in bending DSM and GMNI predict extremely similar capacities.

6.2. Sections with large corner radius

Unlike Eurocode design procedure (with effective widths), the DSM procedure can technically be applied to any cross-section if the elastic critical values are known. Since in our study global buckling is certainly excluded, while distortional buckling is mostly eliminated by the selection of cross-section type or cross-section and member dimensions, it is enough to determine the elastic critical load for the local-plate buckling. For the DSM capacity prediction the local critical load is calculated by finite strip analysis using CUFSM [22]. For sections with large corner radius various local buckling modes exist. The local critical stress is taken as the first minimum point of the signature curve. It is found that in case of large corner radius this local critical stress is relatively sensitive to the applied discretization, therefore a relatively fine cross-section discretization is used. (It is to note that the local critical stress calculated by CUFSM as described above show good coincidence with the lowest critical stress calculated by the FEM model, discussed in Section 2.2 of this paper. The coincidence is especially good for large corner radii.)

The results are summarized in Fig. 13 and Fig. 14 for the hollow and the C-shaped sections, respectively, for two values of large corner radius (namely: 30 and 40 mm). Cases with various thicknesses are presented, thus, the presented results cover a wide range of r/t ratios.

The DSM prediction, in general, is reasonable for the plate-like behaviour, even if the here presented cross-section geometries are mostly out of the domain of pre-qualified sections. In case of SHS in

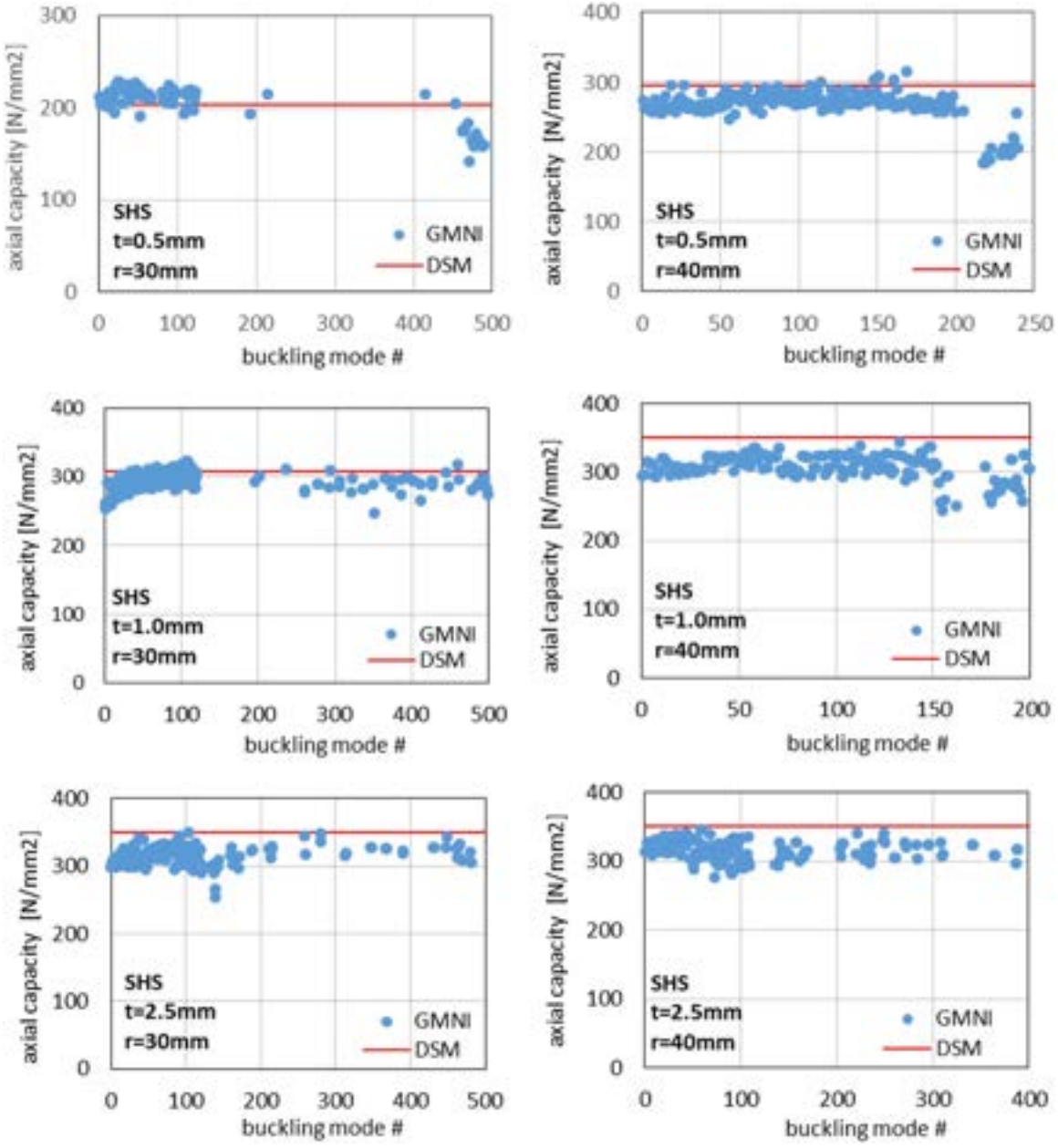

Fig. 13. Capacity prediction for SHS sections with large corner radius.

compression, the DSM prediction seems to be slightly unconservative if compared to GMNI prediction. In case of C sections in bending DSM seems to be either appropriate or slightly conservative (with the exception of the largest r/t ratio). The conservatism of DSM (compared to GMNI) in the case of the $t = 2.5$ mm thickness is most surely comes from the fact that in these cases the section is able to take more loads beyond its elastic capacity due to the partial plastic distribution of stresses, which extra capacity is not acknowledged by DSM but naturally included in GMNI.

If the r/t ratio is large enough, there is a potential for the member to fail well below its plate-like capacity. Clearly, this behaviour is not included in the current DSM prediction.

It is to emphasize that real test results would be necessary to draw more definite conclusions on the capacity of sections with large corner radii.

7. Summary and conclusions

In this paper the buckling behaviour of thin-walled members with cylindrical curved parts is analysed. The objective was to investigate whether cross-sections with large curved parts may behave significantly different compared to regular sections. The focus is on the local buckling behaviour. For this reason parametric studies have been carried out on a shell finite element model with two cross-section topologies, on a double-symmetric hollow section and on a C-like section. The corner radius was systematically increasing from zero to the physically possible maximum. The effect of some other parameters (thickness, geometric imperfection magnitude, imperfection shape, yield strength) has also been examined. The research included linear buckling analysis, as well as elastic and inelastic nonlinear analysis with imperfections. Properly scaled buckling shapes from the linear buckling analysis have been used as equivalent geometric imperfections. The capacities from the materially and geometrically nonlinear analysis analyses were compared to the results calculated by two widely used

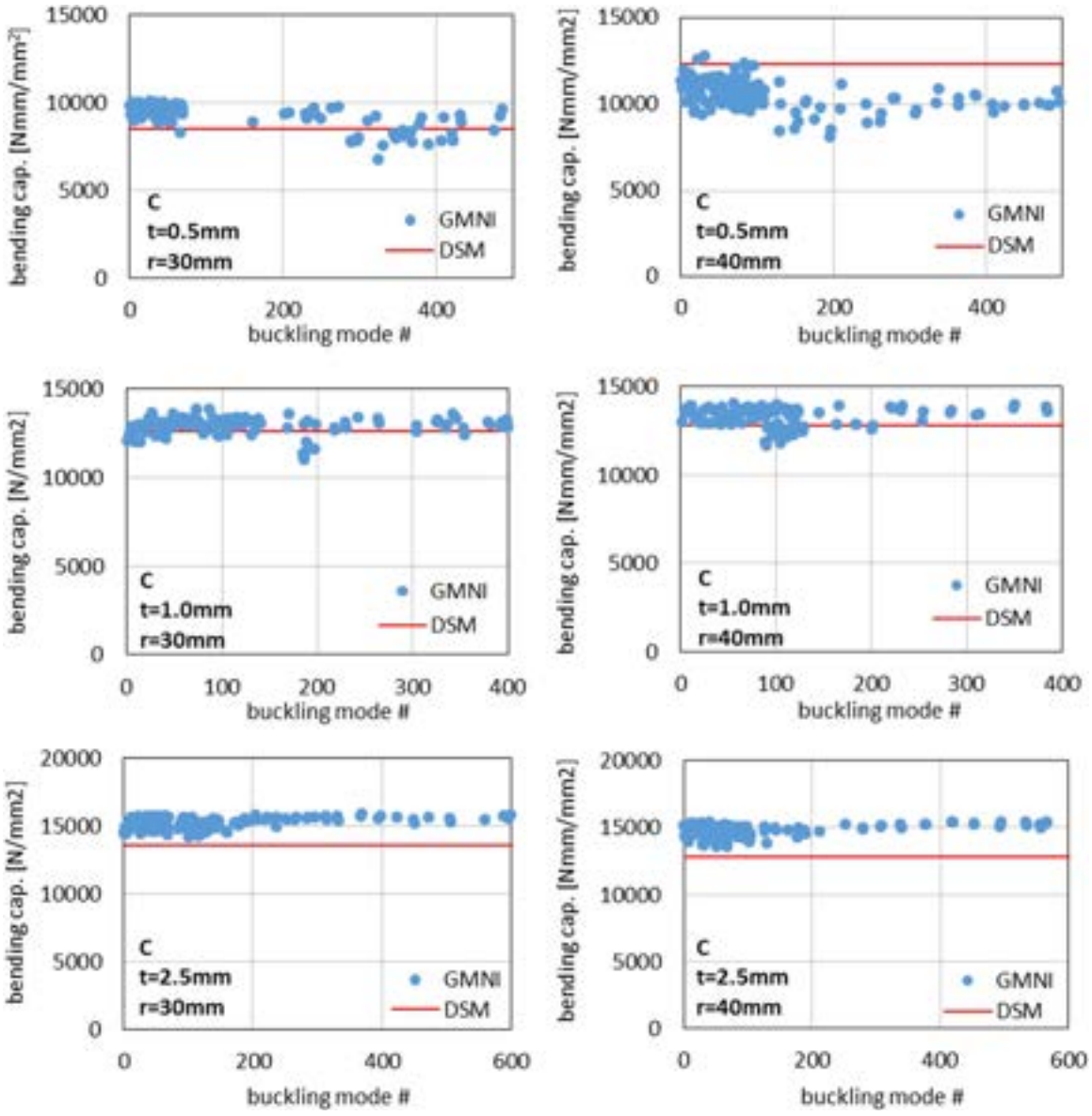

Fig. 14. Capacity prediction for C sections with large corner radius.

design standards: Eurocode 3 and the Direct Strength Method of the North American Specification for cold-formed steel structural members.

The results of the investigations show that cross-sections with large curved parts can be analysed by the Direct Strength Method, and the prediction leads to realistic estimation of the actual local capacity of the member even if the current formulae are used. More research, including real experiments, would be necessary to determine the accuracy of the prediction. It is also shown that the capacities in case of shell-like imperfection shapes might be significantly lower than those In case of plate-like imperfection patterns, which means that shell-like failure of cold-formed steel members can be critical if the corner radius is sufficiently large. More research would be necessary to exactly define when shell-like failure is a potential risk, but the available results suggest that this risk exists if the radius-to-thickness ratio is larger than $20 \div 30$. Anyway, it can clearly be concluded that shell-like failure should be handled in an unconstrained shape optimization process for cold-formed steel members. Finally, it is also clear from the results that large curved parts in cold-formed steel members are beneficial to use, at least from local capacity point of view.

Acknowledgements

The presented work was conducted with the financial support of the OTKA K108912 of the Hungarian Scientific Research Fund and K119440 project of the National Research, Development and Innovation Office.

References

[1] J. Leng, J.K. Guest, B.W. Schafer, Shape optimization of cold-formed steel columns, Thin-Walled Struct. 49 (2011) 1492–1503.
[2] Zhanjie Jiazhen Leng, James K. Li, Benjamin W. Guest, Schafer, shape optimization of cold-formed steel columns with fabrication and geometric end-use constraints, Thin-Walled Struct. 85 (2014) 271–290, http://dx.doi.org/10.1016/j.tws.2014.08.014.
[3] M. Kripka, Z. Martin, Cold-formed steel channel columns optimization with simulated annealing method, Struct. Eng. Mech. 48 (3) (2013) 383–394.
[4] M. Moharrami, A. Louhghalam, M. Tootkaboni, Optimal folding of cold formed steel cross sections under compression, Thin-Walled Struct. 76 (2014) 145–156.
[5] B. Wang, B.P. Gilbert, H. Guan, L.H. Teh, Shape optimisation of manufacturable and usable cold-formed steel singly-symmetric and open columns, Thin-Walled Struct. 109 (2016) 271–284, http://dx.doi.org/10.1016/j.tws.2016.10.004.
[6] B. Wang, B.P. Gilbert, A.M. Molinier, H. Guan, L.H. Teh, Shape optimisation of cold-formed steel columns with manufacturing constraints using the Hough transform, Thin-Walled Struct. 106 (2016) 75–92, http://dx.doi.org/10.1016/j.tws.2016.04.

015.
[7] B. Wang, G.L. Bosco, B.P. Gilbert, H. Guan, L.H. Teh, Unconstrained shape optimisation of singly-symmetric and open cold-formed steel beams and beam-columns, Thin-Walled Struct. 104 (2016) 54–61, http://dx.doi.org/10.1016/j.tws.2016.03.007.
[8] B.P. Gilbert, T.J.M. Savoyat, L.H. Teh, Self-shape optimisation application: optimisation of cold-formed steel columns, Thin-Walled Struct. 60 (2012) 173–184, http://dx.doi.org/10.1016/j.tws.2012.06.008.
[9] B.P. Gilbert, L.H. Teh, H. Guan, Self-shape optimisation principles: optimisation of section capacity for thin-walled profiles, Thin-Walled Struct. 60 (2012) 194–204, http://dx.doi.org/10.1016/j.tws.2012.06.009.
[10] J.F.A. Madeira, J. Dias, N. Silvestre, Multiobjective optimization of cold-formed steel columns, Thin-Walled Struct. 96 (2015) 29–38.
[11] DSM, American Iron and Steel Institute. Direct Strength Method Design Guide. Washington DC, USA, 2006.
[12] A.B. Sabbagh, M. Petkovski, K. Pilakoutas, R. Mirghaderi, Development of cold-formed steel elements for earthquake resistant moment frame buildings, Thin-Walled Struct. 53 (2012) 99–108, http://dx.doi.org/10.1016/j.tws.2012.01.004.
[13] A.B. Sabbagh, M. Petkovski, K. Pilakoutas, R. Mirghaderi, Ductile moment-resisting frames using cold-formed steel sections: an analytical investigation, J. Constr. Steel Res. 67 (4) (2011) 634–646, http://dx.doi.org/10.1016/j.jcsr.2010.11.016.
[14] S. Ádány, D. Jobbágy, A.L. Joó, D. Visy, Stability analysis of thin-walled members with curved cross-section parts: elastic behaviour, in: Proceeding of the International Colloquium on Stability and Ductility of Steel Structures, Timisoara, Romania, May 30–June 1 , 2016, pp. 267–274.
[15] D. Jobbágy, S. Ádány, Stability analysis of thin-walled members with curved cross-section parts: inelastic behavior, in: Proceeding of Recent Research and Developments in Cold-Formed Steel Design and Construction, Baltimore, USA, Nov 9–10, 2016, pp. 89–103.
[16] CEN, EN 1993-1-5:2006 – Eurocode 3: Design of Steel Structures – Part 1–5: Plated Structural Elements, European Committee for Standardization, Brussels, Belgium, 2006.
[17] CEN, EN 1993-1-3:2006 – Eurocode 3: Design of steel structures – Part 1–3: General Rules, Supplementary Rules for Cold-formed Members and Sheeting, European Committee for Standardization, Brussels, Belgium, 2006.
[18] CEN, EN 1993-1-1:2005 – Eurocode 3: Design of steel structures – Part 1–1: General Rules and Rules for Buildings, European Committee for Standardization, Brussels, Belgium, 2005.
[19] NAS, North American Specification for the Design of Cold-formed Steel Structural Members. 2007 ed. Washington DC, USA, American Iron and Steel Institute, 2007.
[20] ANSYS Inc., ANSYS Mechanical, Release 17.1.
[21] CEN, EN 1993-1-6:2007 – Eurocode 3: Design of steel structures – Part 1–6: General Rules – Strength and Staility of Shell Structures, European Committee for Standardization, Brussels, Belgium, 2007.
[22] CUFSM v4.05: Elastic Buckling Analysis of Thin-Walled Members by Finite Strip Analysis, 2012 ⟨http://www.ce.jhu.edu/bschafer/cufsm⟩.